Modeling for V–O_2 reactive sputtering process using a pulsed power supply*

Wang Tao(王 涛)[a)†], Yu He(于 贺)[a)], Dong Xiang(董 翔)[a)],
Jiang Ya-Dong(蒋亚东)[a)], Chen Chao(陈 超)[a)], and Wu Ro-Land(胡锐麟)[b)]

[a)] School of Optoelectronic Information, University of Electronic Science and Technology of China (UESTC), Chengdu 610054, China
[b)] Center for Plasma Material Interaction, Department of Nuclear, Plasma and Radiological Engineering, University of Illinois at Urbana-Champaign, IL, 61801, USA

(Received 1 January 2014; revised manuscript received 13 March 2014; published online 20 June 2014)

In this article, we present a time-dependent model that enables us to describe the dynamic behavior of pulsed DC reactive sputtering and predict the film compositions of VO_x prepared by this process. In this modeling, the average current J is replaced by a new parameter of $J_{\rm eff}$. Meanwhile, the four species states of V, V_2O_3, VO_2, and V_2O_5 in the vanadium oxide films are taken into consideration. Based on this work, the influences of the oxygen gas supply and the pulsed power parameters including the duty cycle and frequency on film compositions are discussed. The model suggests that the time to reach process equilibrium may vary substantially depending on these parameters. It is also indicated that the compositions of VO_x films are quite sensitive to both the reactive gas supply and the duty cycle when the power supply works in pulse mode. The 'steady-state' balance values obtained by these simulations show excellent agreement with the experimental data, which indicates that the experimentally obtained dynamic behavior of the film composition can be explained by this time-dependent modeling for pulsed DC reactive sputtering process. Moreover, the computer simulation results indicate that the curves will essentially yield oscillations around the average value of the film compositions with lower pulse frequency.

Keywords: time-dependent model, pulsed DC reactive sputtering, film composition, duty cycle

PACS: 81.15.Cd, 81.15.Ef **DOI:** 10.1088/1674-1056/23/8/088113

1. Introduction

As a fascinating material with excellent physical and chemical properties, vanadium oxide thin film has been studied extensively.[1,2] The chemical state of V in VO_x ranges from V^{2+} to V^{5+}, which correspond to the form of VO, V_2O_3, VO_2, and V_2O_5, respectively. Therefore, how to adjust film composition according to particular applications is a challenge.

Vanadium oxide thin films have been widely prepared by a reactive magnetron sputtering method.[3] In order to improve the controllability of the reactive sputtering process of VO_x thin films, a variety of novel sputtering methods have been developed, such as pulsed DC reactive magnetron sputtering,[4] RF reactive magnetron sputtering,[5] inductively coupled plasma-assisted reactive sputtering ,[6] and ion beam reactive sputtering,[7] etc. Among these sputtering methods, pulsed DC reactive magnetron sputtering offers significant advantages over others, including excellent arc suppression, low target poisoning, a stable reactive sputtering process, a relatively high deposition rate, flexible process control, and simple apparatus.

The mechanism of reactive sputtering was reasonably well described by the Berg model,[8,9] and recently extensions to this model have been published.[10–15] The static behavior of the V–O_2 reactive sputtering process has previously been carefully investigated.[16] A few attempts to describe the dynamic behavior of the reactive sputtering process have been suggested.[17–19] However, none of the suggested models are able to predict the film composition, which plays a significant role in the film deposition process, especially for multi-component thin films such as vanadium oxides.

In this work, we propose a model for the time-dependent behavior of the V–O_2 reactive sputtering process using a pulsed power supply. The fraction of film compositions is investigated as a function of time t during the reactive sputtering of multi-component thin film. Meanwhile, the influences of the oxygen gas supply and the pulsed power parameters including the duty cycle and frequency on the component fraction at the substrate surface are discussed. One of the most important results of our investigations indicates that there may be substantial differences in the film compositions depending on both the oxygen gas supply and the pulse parameters. Besides, we present results showing the abrupt changes of film composition with respect to reactive gas flow as well as pulse duty cycle.

*Project partially supported by the National Natural Science Foundation of China (Grant Nos. 61071032, 61377063, and 61235006).
†Corresponding author. E-mail: wtwh@uestc.edu.cn
© 2014 Chinese Physical Society and IOP Publishing Ltd

2. Model

The suggested model is the further development of a previously presented model.[16] Unlike the earlier models, both target and substrate are assumed to be covered with V, V_2O_3, VO_2, and V_2O_5. The mathematical model describing the sputtering system is shown in Fig. 1. The total supply rate of the reactive gas (oxygen) is denoted as $Q_{\rm tot}$. In order to simulate this more efficiently, we make some additional assumptions. The same situation exists in the receiving area where all sputtered materials are assumed to be uniformly collected. The target surface can be divided into four parts (see Fig. 1). Here $\theta_{\rm t1}$ is denoted as the fractional area of the target surface that consists of unreacted metal vanadium. The $\theta_{\rm t2}$, $\theta_{\rm t3}$, $\theta_{\rm t4}$ fractions would be assumed to be covered by V_2O_3, VO_2, and V_2O_5, respectively.

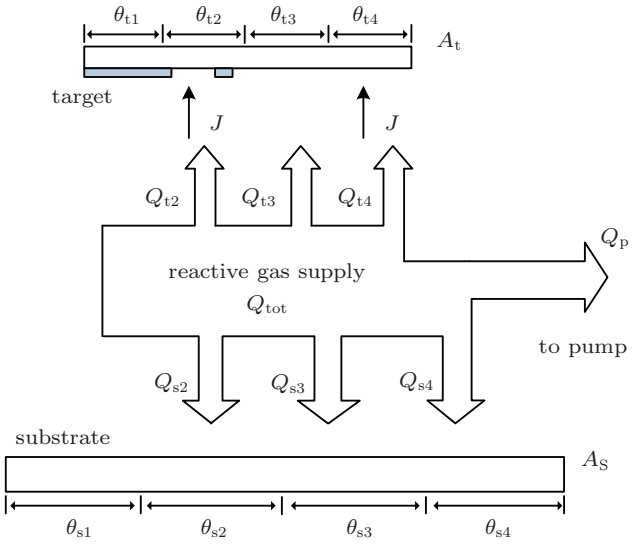


Fig. 1. Schematic diagram of a simple reactive-sputtering system.

2.1. Time-dependent model

According to the kinetic model for reactive sputtering, the time dependence of the compound coverage at target θ is given by

$$\frac{{\rm d}\theta}{{\rm d}t} = \frac{1}{N_0}[V_{\rm f} - V_{\rm g}], \tag{1}$$

where N_0 is the areal density of atoms on the target surface, $V_{\rm g}$ the sputtering rate of compound from target, and $V_{\rm f}$ the forming rate of compound onto target. In the modified model, the equation should be rewritten as

$$\frac{{\rm d}\theta_{\rm t1}}{{\rm d}t} = \frac{1}{N_0}[V_{\rm ft1} - V_{\rm gt1}], \tag{2}$$

$$\frac{{\rm d}\theta_{\rm t2}}{{\rm d}t} = \frac{1}{N_0}[V_{\rm ft2} - V_{\rm gt2}], \tag{3}$$

$$\frac{{\rm d}\theta_{\rm t3}}{{\rm d}t} = \frac{1}{N_0}[V_{\rm ft3} - V_{\rm gt3}], \tag{4}$$

$$\frac{{\rm d}\theta_{\rm t4}}{{\rm d}t} = \frac{1}{N_0}[V_{\rm ft4} - V_{\rm gt4}], \tag{5}$$

$$\frac{{\rm d}\theta_{\rm s1}}{{\rm d}t} = \frac{1}{N_0}[V_{\rm fs1} - V_{\rm gs1}], \tag{6}$$

$$\frac{{\rm d}\theta_{\rm s2}}{{\rm d}t} = \frac{1}{N_0}[V_{\rm fs2} - V_{\rm gs2}], \tag{7}$$

$$\frac{{\rm d}\theta_{\rm s3}}{{\rm d}t} = \frac{1}{N_0}[V_{\rm fs3} - V_{\rm gs3}], \tag{8}$$

$$\frac{{\rm d}\theta_{\rm s4}}{{\rm d}t} = \frac{1}{N_0}[V_{\rm fs4} - V_{\rm gs4}], \tag{9}$$

where $V_{\rm gt1}$–$V_{\rm gt4}$ are the sputtering rates of V, V_2O_3, VO_2, and V_2O_5 from the target, and $V_{\rm ft1}$–$V_{\rm ft4}$ are the forming rates of V, V_2O_3, VO_2, and V_2O_5 onto the target. $V_{\rm gs1}$–$V_{\rm gs4}$ are the consuming rates of V, V_2O_3, VO_2, and V_2O_5 from the substrate, and $V_{\rm fs1}$–$V_{\rm fs4}$ are the forming rates of V, V_2O_3, VO_2, and V_2O_5 onto the substrate.

2.2. Conditions at the target and substrate surface

It is assumed that the capture of reactive gas by metal atoms contributes to the formation of a suboxide V_2O_3 on the substrate, thus increasing $\theta_{\rm s2}$ and reducing $\theta_{\rm s1}$. Further attachment (by oxygen) onto this suboxide V_2O_3 contributes to the formation of the VO_2, thus increasing $\theta_{\rm s3}$, also reducing $\theta_{\rm s2}$. The superoxide V_2O_5 is formed by the reaction between reactive gas and VO_2. For the metal vanadium sputtered from the target, when the metal comes from the fraction of $\theta_{\rm t1}$ placed on the substrate surface which previously consisted of VO_x (V_2O_3, VO_2, and V_2O_5), the fraction of $\theta_{\rm s1}$ will increase and the fraction of $(1-\theta_{\rm s1})$ will decrease. Furthermore, when the VO_x particle sputtered from the target placed on the substrate which previously consisted of VO_i ($i! = x$), then the corresponding fraction of $\theta_{\rm si}$ will decrease and the fraction of VO_x will increase. The fraction of flux $(J/q)Y_{\rm ti}\theta_{\rm ti}A_{\rm t}$ deposited on the fraction $\theta_{\rm si}$ of the collecting area $A_{\rm s}$ will not influence the value of $\theta_{\rm s1}$. Adding elemental non-reacted target atoms to an area that already consists of non-reacted atoms does not change $\theta_{\rm s1}$.

By making the above-mentioned new assumptions in combination with the simplifications presented earlier, the time-dependent balance equations for the conditions on the target should be rewritten as the following equations:

$$\frac{{\rm d}\theta_{\rm t1}}{{\rm d}t} = \frac{1}{N_0}\left[\frac{J}{q}Y_{\rm t2}\theta_{\rm t2}A_{\rm t} + \frac{J}{q}Y_{\rm t3}\theta_{\rm t3}A_{\rm t} + \frac{J}{q}Y_{\rm t4}\theta_{\rm t4}A_{\rm t} - 2\alpha_1 FA_{\rm t}\theta_{\rm t1}/l_2\right], \tag{10}$$

$$\frac{{\rm d}\theta_{\rm t2}}{{\rm d}t} = \frac{1}{N_0}\left[2\alpha_1 FA_{\rm t}\theta_{\rm t1}/l_2 - \frac{J}{q}Y_{\rm t2}\theta_{\rm t2}A_{\rm t} - 2\alpha_2 FA_{\rm t}\theta_{\rm t2}/(l_3 - l_2)\right], \tag{11}$$

$$\frac{{\rm d}\theta_{\rm t3}}{{\rm d}t} = \frac{1}{N_0}\left[2\alpha_2 FA_{\rm t}\theta_{\rm t2}/(l_3 - l_2)\right.$$

$$-\frac{J}{q}Y_{t3}\theta_{t3}A_t - 2\alpha_3 FA_t\theta_{t3}/(l_4-l_3)], \quad (12)$$

$$\frac{d\theta_{t4}}{dt} = \frac{1}{N_0}\left[2\alpha_3 FA_t\theta_{t3}/(l_4-l_3) - \frac{J}{q}Y_{t4}\theta_{t4}A_t\right]. \quad (13)$$

Here, J is the ion-current density; q is the elementary electronic charge; Y_{t2}, Y_{t3}, and Y_{t4} represent the sputtering yields of the V_2O_3, VO_2, and V_2O_5; the values of α_1–α_3 are the probability (sticking coefficient) for the oxygen molecule to react with V, V_2O_3, and VO_2 respectively; A_t is the area of effective target; the values of l_1–l_4 are the stoichiometric values of V, V_2O_3, VO_2, and V_2O_5, respectively; F represents the neutral reactive molecules/(unit area and time).

Meanwhile, the time-dependent balance equations for the conditions on the substrate should be rewritten as the following equation:

$$\begin{aligned}\frac{d\theta_{s1}}{dt} &= \frac{1}{N_0}\left[\frac{J}{q}Y_{t1}\theta_{t1}A_t(1-\theta_{s1})\right.\\ &= \left(\frac{J}{q}Y_{t2}\theta_{t2}A_t + \frac{J}{q}Y_{t3}\theta_{t3}A_t + \frac{J}{q}Y_{t4}\theta_{t4}A_t\right)\theta_{s2}\\ &\quad \left.-2\alpha_1 FA_s\theta_{s1}/l_2\right], \quad (14)\end{aligned}$$

$$\begin{aligned}\frac{d\theta_{s2}}{dt} &= \frac{1}{N_0}\left[\frac{J}{q}Y_{t2}\theta_{t2}A_t(1-\theta_{s2}) + 2\alpha_1 FA_s\theta_{s1}/l_2\right.\\ &\quad -\left(\frac{J}{q}Y_{t1}\theta_{t1}A_t + \frac{J}{q}Y_{t3}\theta_{t3}A_t + \frac{J}{q}Y_{t4}\theta_{t4}A_t\right)\theta_{s2}\\ &\quad \left.-2\alpha_2 FA_s\theta_{s2}/(l_3-l_2)\right], \quad (15)\end{aligned}$$

$$\begin{aligned}\frac{d\theta_{s3}}{dt} &= \frac{1}{N_0}\left[\frac{J}{q}Y_{t3}\theta_{t3}A_t(1-\theta_{s3}) + 2\alpha_{s2}FA_s\theta_{s2}/(l_3-l_2)\right.\\ &\quad -\left(\frac{J}{q}Y_{t1}\theta_{t1}A_t + \frac{J}{q}Y_{t2}\theta_{t2}A_t + \frac{J}{q}Y_{t4}\theta_{t4}A_t\right)\theta_{s3}\\ &\quad \left.-2\alpha_{s3}FA_s\theta_{s3}/(l_4-l_3)\right], \quad (16)\end{aligned}$$

$$\begin{aligned}\frac{d\theta_{s4}}{dt} &= \frac{1}{N_0}\left[\frac{J}{q}Y_{t4}\theta_{t4}A_t(1-\theta_{s4}) + 2\alpha_3 FA_s\theta_{s3}/(l_4-l_3)\right.\\ &\quad \left.-\left(\frac{J}{q}Y_{t1}\theta_{t1}A_t + \frac{J}{q}Y_{t2}\theta_{t2}A_t + \frac{J}{q}Y_{t4}\theta_{t4}A_t\right)\theta_{s4}\right]. \quad (17)\end{aligned}$$

2.3. Effective current for pulsed sputtering

In order to study the effect of pulsed parameters on the reactive sputtering process, an effective target current density J_{eff} is introduced, replacing J in the above equation, as shown in Fig. 2.

As a consequence, the influence of pulsed parameters including the duty cycle and frequency can be investigated by adjusting the values of τ_{on} and τ_{off}. J_{eff} is a function of time t as shown in Fig. 2. $J_{eff}(t)$ is equal to J during the ON period, and is equal to zero during the OFF period. This is the main idea of this modified model. We assume that the sputtering process could only take place during the ON period. Hence, the fraction of flux $(J/q)Y_{ti}\theta_{ti}A_t$ is equal to zero during the OFF period of the pulse. Meanwhile, equations (10)–(17) each are a function of J_{eff}. In this case, the dynamic behavior of film composition is quite sensitive to τ_{on} and τ_{off}.

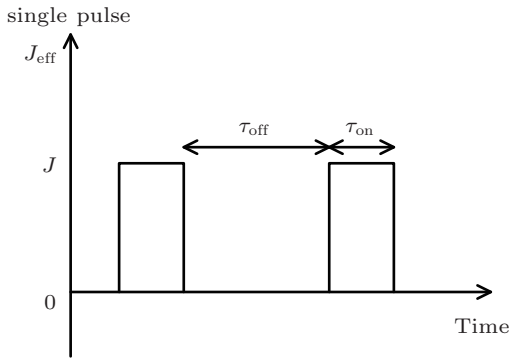


Fig. 2. Time variations of pulsed current density.

2.4. Gettering of the reactive gas

The consumption of the target material Q_t can be expressed as

$$\begin{aligned}Q_{t1} &= 2\alpha_1 FA_t\theta_{t1}/l_2,\\ Q_{t2} &= 2\alpha_2 FA_t\theta_{t2}/(l_3-l_2),\\ Q_{t3} &= 2\alpha_3 FA_t\theta_{t3}/(l_4-l_3),\\ Q_t &= Q_{t2}+Q_{t3}+Q_{t4}. \quad (18)\end{aligned}$$

The consumption of the substrate material Q_s can be expressed as

$$\begin{aligned}Q_{s2} &= 2\alpha_1 FA_s\theta_{s1}/l_2,\\ Q_{s3} &= 2\alpha_2 FA_s\theta_{s2}/(l_3-l_2),\\ Q_{s4} &= 2\alpha_3 FA_s\theta_{s3}/(l_4-l_3),\\ Q_s &= Q_{s2}+Q_{s3}+Q_{s4}. \quad (19)\end{aligned}$$

The remaining part Q_p of the reactive gas will escape from the processing chamber through the pumping system. Assuming the pumping speed is S for the system pump,

$$Q_p = \frac{PN_a}{R_rT}S. \quad (20)$$

In the kinetic model, the partial pressure of the reactive gas P is determined not only by both the reactive gas flow rate fed into the chamber and the flow rate out through pumping, but also by the gettering effect.

$$\frac{dP}{dt} = \frac{Q-Q_t-Q_p}{V_c}. \quad (21)$$

Here, P and Q are the partial pressure and the flow rate of the reactive gas, respectively, V_c is the volume of chamber.

3. Results and discussion

It is possible to experimentally quantify the ratio of components on the substrate in a pulsed reactive sputtering system

by measuring the film compositions under different duty cycles, frequencies, and oxygen flow conditions using XPS analysis. The experimental results of corresponding composition data are shown in Table 1.

Table 1. Experimental results of film composition.

O_2 flow rate/sccm	Duty cycle/%	Peak area ratio/%			
		V^0	V^{3+}	V^{4+}	V^{5+}
3.1	100	21	37	35	7
	80	13	24	49	14
	55	0	12	60	28
3.3	100	13	24	51	12
	80	6	21	43	30
	55	0	0	39	61
3.5	100	10	24	48	18
	80	0	0	40	60
	55	0	0	0	100

The values of all the constants are first adjusted in order to realize the best fitting to the experimental data at the 3.1 sccm with different duty cycles. The optimal values of the constants are $\alpha_1 = 1.8$, $\alpha_2 = 4.7$, $\alpha_3 = 0.35$, $Y_{t1} = 0.8$, $Y_{t2} = 0.8$, $Y_{t3} = 1.2$, and $Y_{t4} = 0.4$. These constant values are then used to predict other conditions of 3.3 sccm and 3.5 sccm. The good agreement is obtained as shown in Figs. 4 and 5, which indicates that the constants are well-calibrated. Based on the model, the fraction of composition on the substrate as a function of time t is calculated. Then, the end values of film composition are recorded in Table 2.

Table 2. Calculated result of film composition.

O_2 flow rate/sccm	Duty cycle/%	Peak Area ratio/%			
		V^0	V^{3+}	V^{4+}	V^{5+}
3.1	100	27	33	32	8
	80	19	23	42	16
	55	0	12	56	32
3.3	100	14	23	50	13
	80	8	19	43	30
	55	0	0	38	62
3.5	100	10	24	48	18
	80	0	0	43	57
	55	0	0	0	100

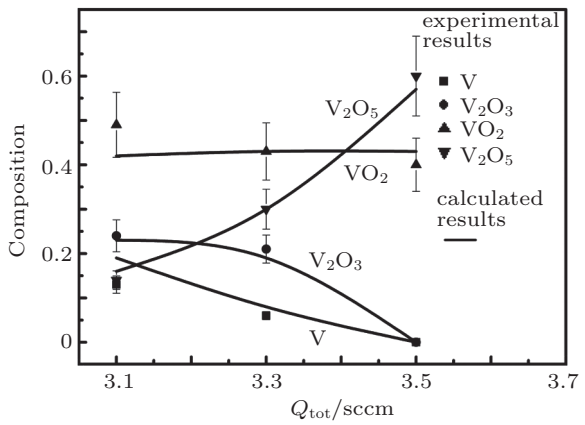


Fig. 3. Comparisons between the experimental and modeling results of film compositions (duty cycle: 80%) each as a function of reactive gas flow (Q_{tot}).

The comparison between the experimental and modeling results of film compositions is shown as a function of reactive gas flow with a duty cycle of 80% in Fig. 3. Also, figure 4 shows the film compositions as a function of each duty cycle. It is found that the errors between experimental and modeling results are all less than 15% over the whole table, and less than 8% for most values. The influences of reactive gas supply, duty cycle, and frequency on film composition will be discussed in detail below.

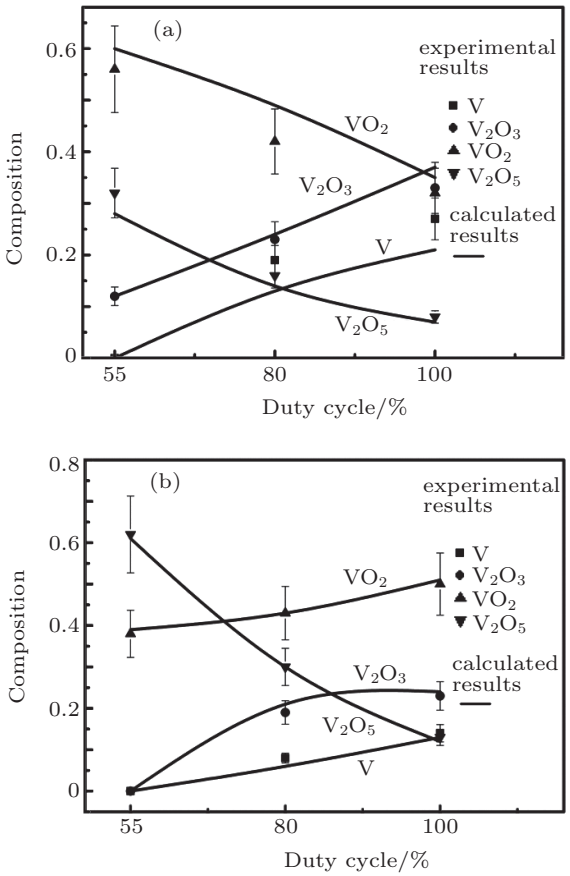


Fig. 4. Comparisons between the experimental and modeling results of film compositions each as a function of duty cycle (D), for (a) $Q_{tot} = 3.1$ sccm and (b) $Q_{tot} = 3.3$ sccm.

3.1. Fractions of components on the substrate

A pulsed DC sequence may be simulated by the new dynamic model. For simplicity we assume a pulse shape, where sputtering is ON in 80% of the duty cycle and the sputtering is OFF in the rest of the period. Here the variations in fractions of V, V_2O_3, VO_2, and V_2O_5 on the substrate with time are shown in Fig. 5. It is assumed that initial compound coverage almost reaches zero. The coverages of compound (V_2O_3, VO_2, and V_2O_5) increase sharply at the beginning, and then gradually increase, finally reaching steady-state conditions. As oxygen flow Q increases, a greater amount of oxygen is consumed by target surface oxidation, leading to an increase in the fraction

of compound on the target. It should also be noted that the content of V_2O_3 increases by approximately 24% while the content of VO_2 increases 43%. However, the content of V_2O_5 is around 14% at the steady state, which is quite low. All these mean that the films contain much more VO_2 than V_2O_3, but less V_2O_5. On the one hand, this is a consequence of the higher reactivity of V_2O_3 than of V with oxygen. On the other hand, the oxygen flow is so low that not enough oxygen can be consumed by VO_2. The experimental results show the similar 'steady-state' balance values to all the above simulation results.

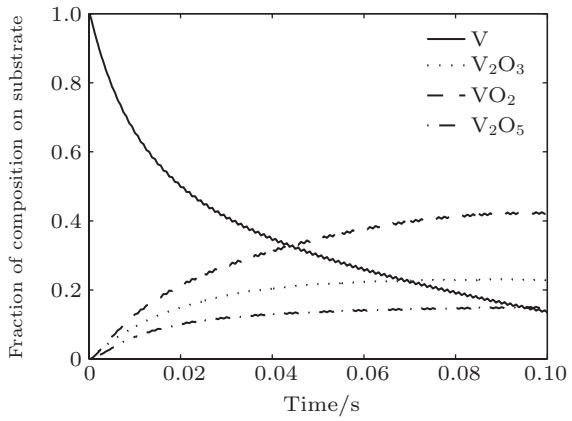


Fig. 5. Variations of the calculated fractions of V, V_2O_3, VO_2, and V_2O_5 on the substrate with time for a pulsed DC reactive sputtering process operating with a reactive gas supply of 3.1 sccm and a duty cycle of 80%.

3.2. Variation of oxygen gas supply

From Table 1, it can be seen that if the process is ON 80% of the duty cycle, the fraction of V_2O_3 is inversely proportional to oxygen flow while the fraction of V_2O_5 is proportional to oxygen flow. With the oxygen flow increasing from 3.1 sccm to 3.3 sccm, the 'steady-state' value of V_2O_3 decreases from 24% to 21%. Continuing to increase the oxygen flow, the fraction of V_2O_3 reaches zero in the steady state. It is seen that the trends of variation in the experimental results are adequately described by the simulation results. It is possible to combine the above equations and solve all the composition fractions of substrate versus time t. From the simulation results obtained, the substrate surface coverage can be estimated. The typical curves of V_2O_3 and V_2O_5 are shown in Figs. 6(a) and 6(b), respectively.

At an oxygen flow rate of 3.1 sccm, the coverage of V_2O_3 at the substrate will gradually increase to a steady-state value of 24%. However, the coverage of V_2O_3 with an oxygen flow rate of 3.3 sccm will gradually increase to about 31% at 0.04 s. It should also be noted that there is a short decrease in the fraction of V_2O_3 in the region from 0.04 s to 0.1 s. For an oxygen flow rate of 3.5 sccm, the fraction of V_2O_3 increases to about 7% at the beginning, then abruptly decreases and eventually disappears. There are several reasons explaining these curves. For a low flow rate of oxygen, the supply of the reactive gas is too low to react with V_2O_3. In this case, the fraction of V_2O_3 will increase asymptotically. While at a higher flow rate of oxygen (3.3 sccm), the reaction of V_2O_3 and the gas supply will contribute to a small reduction of V_2O_3. This is a consequence of the higher reactivity of V_2O_3 than that of V with oxygen. At 3.5 sccm, the amount of O_2 consumed to V_2O_3 exceeds the amount of O_2 gettered by deposited V, resulting in a drastic increase in the fraction of V_2O_3. Figure 6(b) shows the variations of the fraction of V_2O_5 with time for different oxygen flow rates. The fractions equal the steady-state values of 14%, 30%, and 58% with oxygen supply rates of 3.1 sccm, 3.3 sccm, and 3.5 sccm, respectively, which has also been seen in the experimental data. As oxygen flow Q rate increases, a bigger amount of oxygen is consumed by substrate surface oxidation, resulting in an increase in the fraction of V_2O_5 at the substrate.

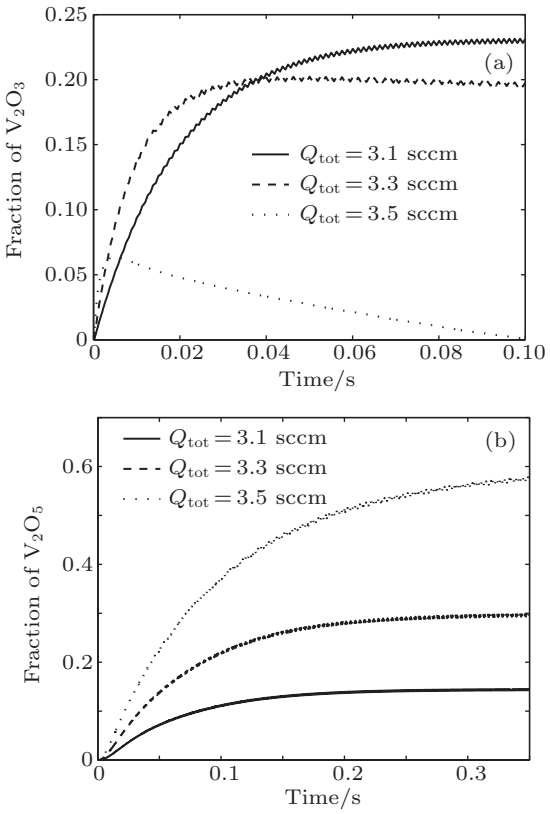


Fig. 6. Time variations of the fractions of film composition for (a) V_2O_3 and (b) V_2O_5 for a pulsed DC reactive sputtering process operating with different gas flow rates in a duty cycle of 80%.

3.3. Variation of the duty cycle

In Table 1, the compositions of VO_x films are found to be strongly dependent on the duty cycle when the power supply works in pulse mode. Figure 7 shows the simulated varia-

tions of the substrate compositions for different duty cycles of pulse. Comparisons between the influences of duty cycle on the surface composition of VO_x thin film with different oxygen flows are also provided in Fig. 7. If film deposition is carried out with an oxygen flow rate of 3.1 sccm, the fractions of V_2O_3, VO_2, and V_2O_5 each as a function of time t are shown in Figs. 7(a), 7(c), and 7(e) respectively. It takes a certain minimum time to build up the steady-state compound layer at the substrate surface depending on what is contained in the layer. In the modeling section, we assume that the gettering of reactive gas onto metal contributes to the formation of a suboxide V_2O_3. Further attachment onto this V_2O_3 contributes to the formation of the VO_2 and the V_2O_5 is formed by the reaction between the oxygen and VO_2. Under this assumption, it is found that the fraction of V_2O_3 reaches its steady-state value after approximately 0.03 s while neither the VO_2 nor V_2O_5 layer comes to its steady-state fraction after approximately 0.04 s and 0.06 s, respectively. Furthermore, reduction of the duty cycle from 100% to 55% leads to a significant decrease of the amount of V^{3+} in contrast to the increase of V^{4+} and V^{5+}. It is seen that at high duty cycle the sputter erosion rate, however, will be so high that the supply of the reactive gas is insufficient to react with V^{3+}, resulting in the lower fraction of V^{4+}. Unlike the condition of 3.1 sccm, it should be noted that with an oxygen flow rate of 3.3 sccm, the reduction of the duty cycle from 100% to 55% contributes to an increase of the steady-state value of V^{4+}. The reason is as follows. At 3.3 sccm, the amount of O_2 consumed to VO_2 exceeds the amount of O_2 gettered by deposited V_2O_3, resulting in a decrease in the fraction of VO_2. Moreover, more reactive gas will be consumed by VO_2 as the oxygen flow rate increases.

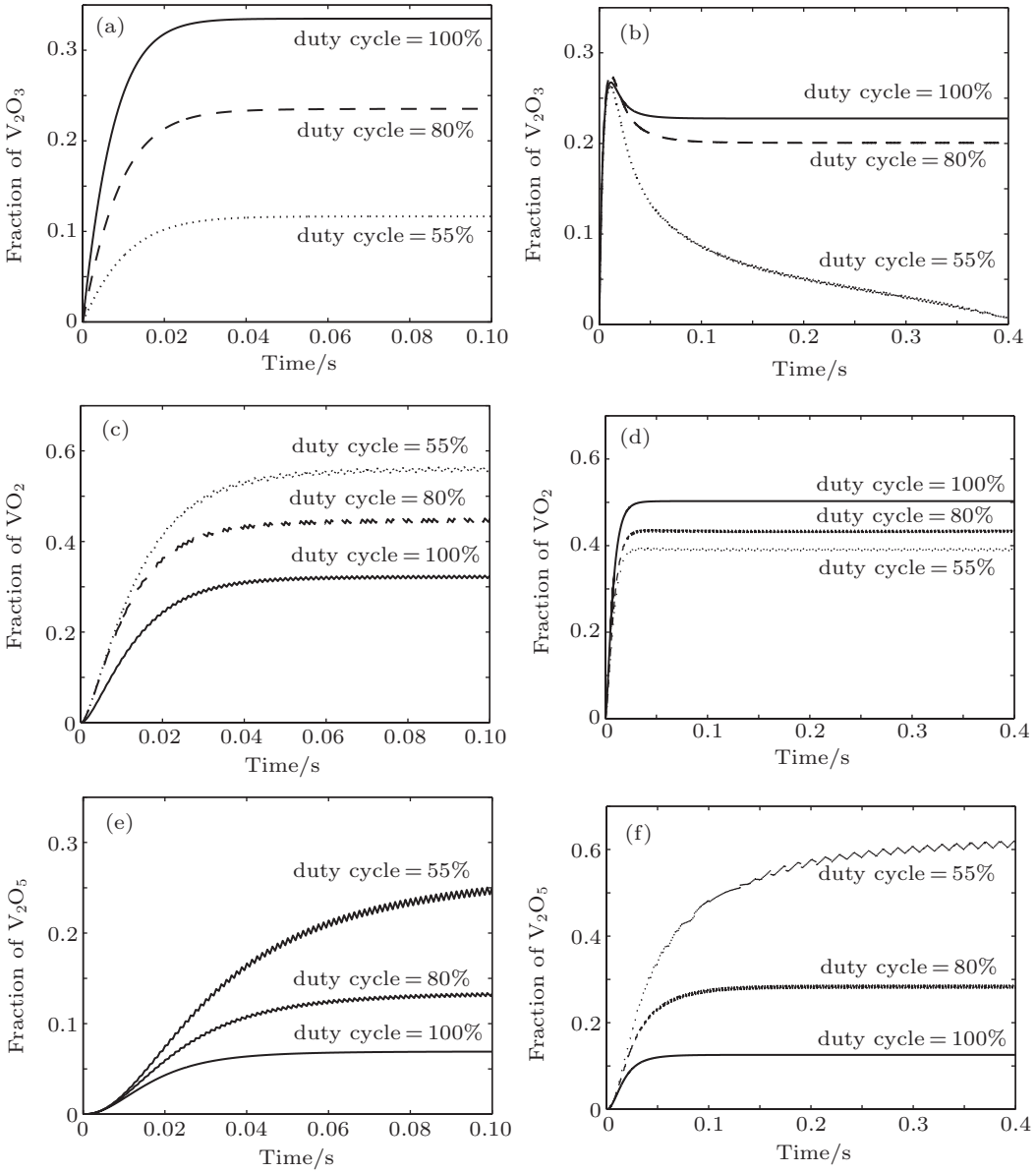


Fig. 7. Time variations of the fractions of V_2O_3, VO_2, and V_2O_5 for a pulsed DC reactive sputtering process operating with different duty cycles with an oxygen flow rate of 3.1 sccm [(a), (c), (e)], and 3.3 sccm [(b), (d), (f)].

The fractions of V_2O_3, VO_2, and V_2O_5 each as a function of time t at 3.3 sccm are shown in Figs. 7(b), 7(d), and 7(f) respectively. It is shown that at higher oxygen gas supply, the coverage of V_2O_3 will gradually increase to about 28% at 0.01 s and then an abrupt decrease occurs in a region from 0.01 s to a certain point depending on the value of duty cycle. For a duty cycle of 55%, the fraction of V_2O_3 decreases to about 8% at the beginning and disappears eventually. At lower duty cycle, the pulse OFF time is long enough for the reaction between the supply of the reactive gas and V_2O_3. Like the group curves of Figs. 7(a), 7(c), and 7(e), it takes significantly longer for the fraction of V_2O_5 to reach a steady state. The 'steady-state' balance values obtained by these simulations are in good agreement with the experimental data seen in Table 1. The nice correlation between the calculated and the experimental curves indicates that the suggested dynamic model is indeed capable of predicting the transient behavior of the pulsed DC reactive sputtering process.

3.4. Variation of the frequency

For a constant gas flow and duty cycle of the pulse, time variations of the fraction of vanadium metal for a pulsed DC reactive sputtering process operating with different frequencies are shown in Fig. 8. It is seen that at each of the low frequencies the metal vanadium will react with the oxygen gas during the negative part of the frequency duty cycle. During the positive part of the duty cycle the sputter erosion rate, however, will be so high that the supply of the oxygen gas is insufficient to react with all sputtered metal vanadium. Therefore, the deposition will approach to being a metallic deposition during this part of the duty cycle. As the frequency increases, however, the time period will be so short that the change in the fraction of the compound on the substrate during one duty cycle becomes negligible. In this case, the oscillations around the average value will decrease significantly as the pulse frequency is increased. Obviously, no oscillations of the chemical composition of the deposited film will take place at frequencies > 800 Hz. In the high frequency mode of operation the fraction of metal vanadium at the substrate will approach to 85%. This value is identical to the value that is obtained if the process is operated in continuous DC reactive sputtering mode.

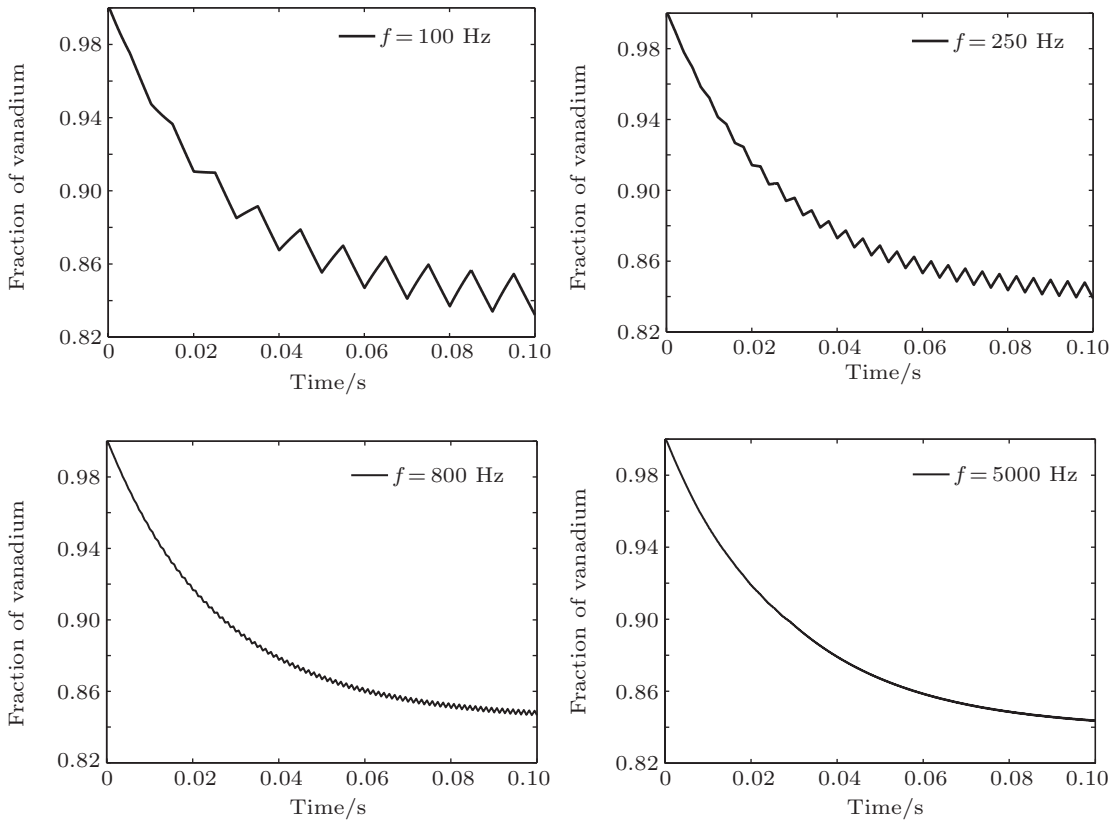


Fig. 8. Time variations of the fractions of V, V_2O_3, VO_2, and V_2O_5 for a pulsed DC reactive sputtering process operating with different frequencies.

4. Conclusion

In this paper we present a model for the time-dependent V–O_2 pulsed DC reactive sputtering process behavior. In this model, the states of four species of V, V_2O_3, VO_2, and V_2O_5 in the vanadium oxide films are taken into consideration. The fraction of film composition is investigated as a function of time t during the reactive sputtering of multi-component thin film. Meanwhile, the influences of the oxygen gas supply and the pulsed power parameters, including the duty cycle and the frequency on the content fractions of the substrate surface, are discussed. The simulation results indicate that film compositions are sensitive to the oxygen gas supply, however, do not show a linear increasing relationship nor linear decreasing relationship. Besides, the compositions of VO_x films are found to be strongly dependent on the duty cycle when the power supply works in pulse mode. It takes a certain minimum time to build up the steady-state compound layer at the substrate surface, depending on what is contained in the layer. The 'steady-state' balance values obtained by these simulations show excellent agreement with the experimental data, which indicates that the experimentally obtained dynamic film composition behavior can be explained by this time-dependent pulsed DC reactive sputtering process. Moreover, the computer simulations indicate that the oscillations around the average value of the film compositions will decrease significantly as the pulse frequency increases.

References

[1] Wei X J, Liang C J, Guang K P, De H, Nie Y X, Zhu S Q, Huang F, Zhang W W and Zheng W 2008 *Chin. Phys. B* **17** 3512
[2] Wei X J and Nie Y X 2002 *Chin. Phys.* **11** 737
[3] Schlag J and Scherber W 2000 *Thin Solid Films* **366** 28
[4] Fieldhouse N, Pursel M S, Horn W M and Bharadwaja N S 2009 *J. Phys. D: Appl. Phys.* **42** 055408
[5] Miyazaki H and Yasui I 2006 *J. Phys. D: Appl. Phys.* **39** 2220
[6] Nihei Y, Sasakawa Y and Okimura K 2008 *Thin Solid Films* **516** 3572
[7] Yi X J, Chen C H, Liu L Q, Wang Y R, Xiong B F, Wang H C and Chen S H 2003 *Infrared Phys. Technol.* **44** 137
[8] Berg S and Nyberg T 2005 *Thin Solid Films* **476** 215
[9] Jonsson B L, Nyberg T and Berg S 2000 *J. Vac. Sci. Technol. A* **18** 503
[10] Depla D, Chen Z Y, Bogaerts A, Ignatova V, Gryse D R and Gijbels R 2004 *J. Vac. Sci. Technol. A* **22** 1524
[11] Depla D, Heirwegh S, Mahieu S, Haemers J and Gryse D R 2007 *J. Appl. Phys.* **101** 013301
[12] Depla D, Heirwegh S, Mahieu S and Gryse D R 2007 *J. Phys. D: Appl. Phys.* **40** 1957
[13] Kubart T, Depla D, Martin M D, Nyberg T and Berg S 2008 *Appl. Phys. Lett.* **92** 221501
[14] Kubart T, Jensen J, Nyberg T, Lijeholm L, Depla D and Berg S 2009 *Vacuum* **83** 1295
[15] Kubart T, Trinh H D, Lijeholm L, Hultman L, Hogberg H, Nyberg T and Berg S 2008 *J. Vac. Sci. Technol. A* **26** 565
[16] Yu H, Jiang Y D, Wang T, Wu Z M, Yu J S and Wei X B 2010 *J. Vac. Sci. Technol. A* **28** 466
[17] Wang T, Jiang Y D, Yu H, Wu Z M and Zhao H N 2011 *Chin. Phys. B* **20** 038101
[18] Kusano E 1993 *J. Appl. Phys.* **73** 8565
[19] Kusano E and Kinbara A 2000 *J. Appl. Phys.* **87** 2015